

UC San Diego

UC San Diego Previously Published Works

Title

D-D mixing in heavy quark effective field theory; the sequel

Permalink

<https://escholarship.org/uc/item/8xt3852k>

Journal

Nuclear Physics B, 403(3)

ISSN

0550-3213

Authors

Ohl, Thorsten
Ricciardi, Giulia
Simmons, Elizabeth H

Publication Date

1993-08-01

DOI

10.1016/0550-3213(93)90364-u

Peer reviewed

#HUTP-92/A053

12/92

hep-ph/9301212

D - \bar{D} Mixing in Heavy Quark Effective

Field Theory: The Sequel

Thorsten Ohl

Giulia Ricciardi

Elizabeth H. Simmons

Lyman Laboratory of Physics*

Harvard University

Cambridge, MA 02138

Abstract

We perform a quantitative analysis of D^0 - \bar{D}^0 mixing in Heavy Quark Effective Field Theory (HqEFT) including leading order QCD corrections. We find an enhancement of the short-distance contribution by a factor of two or three.

*electronic mail addresses: {ohl,ricciardi,simmons}@physics.harvard.edu

1 Introduction

The mixing of neutral particles with their antiparticles through flavor changing neutral currents is a sensitive probe of flavor physics. Ever since the K_L^0 - K_S^0 mass difference was used to predict the charm quark mass [1], these systems have been used to test the standard model and to search for signs of new physics. Recently, there has been interest in D^0 - \bar{D}^0 mixing as a window into dynamical symmetry breaking mechanisms [2, 3, 4].

The traditional analysis of D^0 - \bar{D}^0 mixing in the standard model is plagued by large uncertainties. While the “short distance” contributions are known to be small, it has been argued [5, 6] that the “dispersive” contributions from second-order weak interactions with mesonic intermediate states may be considerably larger. This differs substantially from the situations in the K^0 - \bar{K}^0 and B^0 - \bar{B}^0 systems. In the former, the short distance contributions are expected to be of the same size as the dispersive contribution [7]; in the latter, dispersive effects are expected to be negligible [6].

It has recently been argued [4] that Heavy Quark Effective Field Theory (HqEFT) [8, 9] and naive dimensional analysis [10] suggest that the dispersive contributions are smaller than previously estimated, implying that cancellations occur between contributions from different classes of intermediate mesonic states. In this paper, we perform a quantitative analysis of D^0 - \bar{D}^0 mixing in the HqEFT framework in order to test that assertion. We first calculate the matching contributions at the charm quark scale where the charm quark is removed from the effective theory, leaving only a heavy color charge. Then, we calculate the one-loop anomalous dimensions that contribute to the running of the operators between the charm mass and Λ_{QCD} . Although the

change in scale is not large, a great many operators contribute and there is the possibility that some of them can get a large anomalous dimension.

After describing the effective field theory framework in section 2, we elaborate on the matching conditions and introduce the operator basis for the Wilson expansion in section 3. Then we calculate the one-loop anomalous dimensions for these operators and use the renormalization group equation to pick up the additional contributions from the running between the charm scale and the hadronic scale $\sim \Lambda_{QCD}$ in section 4 and 5. Our numerical results appear in section 6 and our conclusions are presented in section 7.

2 The Effective Field Theory

We shall need to move from the full standard model at high energies to a low-energy effective theory of neutral D meson mixing. Since the D^0 meson is a $\bar{c}u$ state and the CKM (Cabibbo-Kobayashi-Maskawa) matrix element V_{ub} is very small, we shall ignore the effects of the third quark generation altogether. As we pass below the scale $\mu = M_W$, we integrate out the heavy weak bosons and match onto a theory with four-fermion weak interaction operators; this and the subsequent renormalization group running is done in the standard way and introduces nothing surprising. The first really interesting physics comes in at the charm quark threshold: at this point we remove the charm quark from our theory and replace it by a heavy color charge in the HqEFT. We recognize that assuming that m_c lies far enough above Λ_{QCD} for HqEFT to properly capture the charm quark's low energy behavior is questionable. However, we feel that the benefits of approaching the calculation in this way

make the risks worthwhile. And, as one usually says in applying HqEFT to the charm quark, the approximation is well-defined and the corrections are systematically calculable.

At this point, let us remind the reader of some of the essential physics of HqEFT. The central idea is that a system composed of a single heavy quark Q (where “heavy” means $M_Q \gg \Lambda_{QCD}$) and one or more light quarks can be described as a heavy color charge surrounded by generic “brown muck” with the characteristic energy scale of the confining QCD interactions. The mass and velocity of the whole system are essentially identical to those of the heavy quark; the “brown muck” carries only residual momenta of the order of $\Lambda_{QCD} \ll M_Q$. Further, if only QCD interactions are included, the velocity of the heavy quark is constant; additional (e.g.) weak interactions must be included to change the heavy quark velocity.

The most common application of the HqEFT draws upon the fact that the spin and flavor of the heavy quark are decoupled from the brown muck. This enables one to relate decays of various B and D mesons to one another using the HqEFT formalism.

Our reason for using the HqEFT is rather different - what interests us is that no large momentum (e.g. no momentum as large as m_c) can be transferred to the brown muck. This has the surprising consequence that below $\mu = m_c$ charm-changing non-leptonic decays of the neutral D meson are forbidden: such decays would inevitably transfer the large charm quark momentum to light colored degrees of freedom. In other words, no new operators contributing to D^0 - \bar{D}^0 mixing appear at scales below the charm scale! Other than operators arising from short-distance physics (such as W exchange in the familiar box diagrams) the only operators contributing

to D^0 - \bar{D}^0 mixing arise in the matching of the ordinary charm quark onto the heavy charm quark at $\mu = m_c$. So if the HqEFT can really be applied to the c quark, we can calculate the size of D^0 - \bar{D}^0 mixing in the standard model by computing only short distance, matching and running effects.

We should stress some peculiar features of our effective theory. Removing the charm quark from the theory leaves a hard momentum $p \approx m_c > \Lambda_{QCD}$ flowing through the Feynman diagrams for the D^0 - \bar{D}^0 mixing operators. This large momentum forces the internal light quark and gluon propagators far off shell, making it possible to match them with local terms at the charm quark scale. However, in contrast to the W , the light quarks and gluons have not been integrated out: light quarks and gluons with momenta of the order of Λ_{QCD} are still present in our effective theory. It is also crucial to note in the context of D^0 - \bar{D}^0 mixing, that there are no truly “long-distance” contributions to the matching at the scale $\mu \approx m_c$. Because we are matching at a relatively large scale $\mu > \Lambda_{\chi SB}$, quark loops give a good approximation to the sum over all intermediate states. The diagrams of the form shown in figs. 1, 2, and 3 give rise to local four-quark, six-quark, and eight-quark operators below the matching scale.

3 Matching

At the W mass scale, the familiar $\Delta C = 1$ effective hamiltonian can be written in the compact form [4]:

$$H_{eff} = \frac{4G_F}{\sqrt{2}} \left(\bar{\psi}_L \gamma_\mu u_L \right) (\vec{k} \cdot \vec{\tau}) (\bar{c}_L \gamma^\mu \psi_L) \quad (1)$$

where ψ and $\vec{\kappa}$ are respectively:

$$\psi = \begin{pmatrix} s \\ d \end{pmatrix}, \quad \vec{\kappa} = \frac{1}{2} \begin{pmatrix} \cos^2 \theta - \sin^2 \theta \\ -i \\ 2 \cos \theta \sin \theta \end{pmatrix} \quad (2)$$

The subscript L denotes application of the left-handed projection operator $(1 - \gamma^5)/2$; the $\vec{\tau}$ are the Pauli matrices; θ is the Cabibbo mixing angle.

In this section, we will find the coefficients of the four-, six-, and eight-quark operators generated by matching at the charm scale. The four-quark operators come from one-loop matching; the six- and eight-quark operators are generated at tree-level. Although the latter are non leading in $1/m_c$, naive dimensional analysis [4, 10] shows that their matrix elements make important contributions to D^0 - \bar{D}^0 mixing.

3.1 Construction of the Operator Basis

We start by constructing a basis for the multi-quark operators arising from the matching and the operators that mix with them through QCD interactions. Each operator contains two (heavy) charm quarks and an even number of light quarks.

Let us establish some conventions for writing down our multi-quark operators. A $2n$ -quark operator can be written as the product of n currents; we shall always write the current containing a charm anti-quark last and that containing a heavy charm quark next-to-last. So the form of the operators

engendering $\bar{D}^0 \rightarrow D^0$ transitions will be¹

$$\text{four-quark: } (\bar{c}_v \Gamma_1 u) (\bar{\underline{c}}_v \Gamma_2 u) \quad (3)$$

$$\text{six-quark: } (\bar{\psi} \Gamma_1 u) (\bar{c}_v \Gamma_2 \psi) (\bar{\underline{c}}_v \Gamma_3 u) \quad (4)$$

$$\text{eight-quark: } (\bar{\psi} \Gamma_1 u) (\bar{\psi} \Gamma_2 u) (\bar{c}_v \Gamma_3 \psi) (\bar{\underline{c}}_v \Gamma_4 \psi) \quad (5)$$

where each matrix Γ contains the color and Dirac structure of the associated current. Now that we have established the positions that the different quarks occupy in the operators, we can move to a more compact notation which omits the quarks altogether and retains only the Γ matrices

$$\left(\prod_{i=1}^{n-2} \bar{q} \Gamma_i q \right) (\bar{c}_v \Gamma_{n-1} q) (\bar{\underline{c}}_v \Gamma_n q) \mapsto \left(\bigotimes_{i=1}^{n-2} \Gamma_i \right) \otimes \Gamma_{n-1} \otimes \Gamma_n. \quad (6)$$

Here q stands for the appropriate light (u , d , or s) quark. We also recognize that the color and Dirac parts of each Γ factorize. Hence our tensor product notation can be usefully broken down into separate color and Dirac tensor products:

$$\left(\bigotimes_{i=1}^n \Gamma_i \right) = \left(\bigotimes_{i=1}^n \Gamma_i^C \right) \otimes \left(\bigotimes_{i=1}^n \Gamma_i^D \right).$$

¹Following the notation of [4, 9], we distinguish between the charm quark annihilation operator

$$c_v(x) = \frac{1 + \not{v}}{2} e^{im_c v x} c(x)$$

and the anti-charm quark creation operator

$$\underline{c}_v(x) = \frac{1 - \not{v}}{2} e^{-im_c v x} c(x)$$

We have to add the effects of the hermitian conjugates of (3-5) to get the full $\Delta C = 2$ contribution.

From here on, we distinguish the tensor products in color (\otimes_C) and Dirac (\otimes_D) space by subscripts, and we reserve the unqualified tensor product symbol \otimes for the tensor product of color and Dirac space.

The factorization of the Γ matrices implies that the construction of the operator basis naturally divides into two parts. Finding a basis in color space is conceptually simple because all the quarks have the same color properties. One just enumerates all singlets in the tensor product of n copies of $1 \oplus (N^2 - 1)$. We shall see that this is trivial when $n = 2$ or 3 and is not much more complicated for $n = 4$.

Finding a basis in Dirac space is more interesting since the charm and light quarks have different Dirac properties. Since we are calculating to lowest nonvanishing order in the light quark masses, the full standard model theory tells us that the light quarks participating in D^0 - \bar{D}^0 mixing are left-handed:

$$(1 + \gamma^5)q = 0 . \tag{7}$$

According to the HqEFT, the heavy charm quarks are static color sources that do not have a ‘handedness’. What they do have are equations of motion that must be satisfied:

$$(\not{\psi} - 1)c_v = 0 \tag{8}$$

$$(\not{\psi} + 1)\underline{c}_v = 0 \tag{9}$$

and these will affect the Dirac structure of the operator basis. The vector space of the Dirac operators

$$\left(\bigotimes_{i=1}^n \Gamma_i^D \right) \tag{10}$$

for which we want to find a basis is, in fact, a subspace of the n -fold tensor product

$$\mathcal{G}_n = \bigotimes_{i=1}^n \mathcal{G}_1 \quad (11)$$

of the full Dirac algebra \mathcal{G}_1 . The algebra \mathcal{G}_1 is spanned by the usual Minkowski space basis $\{\mathbf{1}, \gamma_\mu, \sigma_{\mu\nu}, \gamma_\mu\gamma^5, \gamma^5\}$. The trick is to define precisely *which* subspace it corresponds to. Since all Lorentz indices in (10) are fully contracted, (10) belongs to the subspace of \mathcal{G}_n that transforms as a scalar under the proper Lorentz group; we call this subspace \mathcal{G}_n^0 . Now if (10) spanned \mathcal{G}_n^0 , in order to find a basis we would only need to extend the usual inner product on \mathcal{G}_1

$$(\Gamma, \Gamma') = \frac{1}{4} \text{Tr}(\Gamma^\dagger \Gamma') \quad (12)$$

to an inner product on \mathcal{G}_n^0

$$(\Gamma, \Gamma') = \prod_{i=1}^n \frac{1}{4} \text{Tr}(\Gamma_i^\dagger \Gamma'_i). \quad (13)$$

Then a basis of (10) could be constructed by finding a complete set orthogonal with respect to the inner product (13). However, the peculiar properties of the currents connecting heavy and light quarks as summarized in (7) and (8-9) mean that the basis vectors of \mathcal{G}_n^0 whose construction we have just described are not independent.

Now we can finish the construction of the basis for the operators (10). We can use the right and left projection operators

$$\pi_r = \bigotimes_{i=1}^n \frac{1}{2} (1 - \gamma^5) \quad (14)$$

$$\pi_l = \left(\bigotimes_{i=1}^{n-2} \frac{1}{2} (1 - \gamma^5) \right) \otimes \frac{1}{2} (1 + \psi) \otimes \frac{1}{2} (1 - \psi) \quad (15)$$

to project onto the subspace of operators with non vanishing matrix elements. Then the kernel of the combined action of these projection operators

$$\{\Gamma \in \mathcal{G}_n^0 | \pi_l \Gamma \pi_r = 0\}$$

is the physically irrelevant portion of \mathcal{G}_n^0 . Therefore the elements of the factor space

$$\overline{\mathcal{G}_n} = \mathcal{G}_n^0 / \{\Gamma \in \mathcal{G}_n^0 | \pi_l \Gamma \pi_r = 0\} \quad (16)$$

correspond to the physically inequivalent operators in which we are interested. $\overline{\mathcal{G}_n}$ can naturally be equipped with an inner product by

$$\overline{(\Gamma, \Gamma')} = \prod_{i=1}^n \frac{1}{4} \text{Tr} \left(\Gamma_i^\dagger \pi_l \Gamma'_i \pi_r \right). \quad (17)$$

The construction of a basis in $\overline{\mathcal{G}_n}$ is now equivalent to finding a maximal subspace of \mathcal{G}_n^0 , such that $\overline{(\cdot, \cdot)}$ is non-degenerate.

3.2 Four-Quark Operators

The basis for the four-quark operators is particularly simple. In color space the only possible operators are the tensor product of a pair of color singlets or a pair of color octets

$$\tau^4_1 = \mathbf{1} \otimes_C \mathbf{1} \quad (18)$$

$$\tau^4_2 = T_a \otimes_C T_a. \quad (19)$$

The Dirac space $\overline{\mathcal{G}_2}$ is spanned by

$$\Upsilon^4_1 = \gamma_L^\mu \otimes_D \gamma_{L,\mu} \quad (20)$$

$$\Upsilon^4_2 = \mathbf{1}_L \otimes_D \mathbf{1}_L. \quad (21)$$

Let us show explicitly how conditions (7) and (8-9) are used to reduce \mathcal{G}_2^0 to (20,21). First, condition (7) selects the left handed sector $\{\mathbf{1}_L, \gamma_{L,\mu}, \sigma_{L,\mu\nu}\}$ of \mathcal{G}_1 . Applying conditions (8-9) removes operators containing ψ or $v_\mu \sigma_L^{\mu\nu}$ from the basis:

$$\begin{aligned}\psi_L \otimes_D \psi_L &= -\Upsilon^4_2 \\ v_\mu \sigma_L^{\mu\nu} \otimes_D \gamma_{L,\nu} &= i\Upsilon^4_1 + i\Upsilon^4_2 \\ \gamma_{L,\nu} \otimes_D v_\mu \sigma_L^{\mu\nu} &= -i\Upsilon^4_1 - i\Upsilon^4_2 \\ v_\mu \sigma_L^{\mu\rho} \otimes_D v_\nu \sigma_{L,\rho}^\nu &= \Upsilon^4_1 + \Upsilon^4_2.\end{aligned}$$

The self duality relation

$$\sigma_L^{\mu\nu} = -\frac{i}{2} \varepsilon^{\mu\nu\kappa\lambda} \sigma_{L,\kappa\lambda} \quad (22)$$

makes operators containing contractions of σ_L and ε redundant and leads to

$$\sigma_{L,\alpha}^\mu \otimes_D \sigma_{L,\nu\alpha} - \sigma_{L,\nu\alpha} \otimes_D \sigma_L^{\mu\alpha} = -i\varepsilon^{\mu\nu\kappa\lambda} \sigma_{L,\kappa\alpha} \otimes_D \sigma_{L,\lambda}^\alpha \quad (23)$$

$$\sigma_{L,\alpha}^\mu \otimes_D \sigma_{L,\nu\alpha} + \sigma_{L,\nu\alpha} \otimes_D \sigma_L^{\mu\alpha} = \frac{1}{2} g^{\mu\nu} \sigma_L^{\kappa\lambda} \otimes_D \sigma_{L,\kappa\lambda}. \quad (24)$$

Finally, contracting (24) with $v_\mu v_\nu$ and using (8-9), we arrive at

$$\sigma_L^{\kappa\lambda} \otimes_D \sigma_{L,\kappa\lambda} = 4 \cdot (\Upsilon^4_1 + \Upsilon^4_2)$$

which leaves us with (20,21) as our basis.

We can now calculate the matching condition at $\mu \approx m_c$ from the one loop diagram in fig. 1.

$$\begin{aligned}&\left(-i4 \frac{G_F}{\sqrt{2}} \sin\theta \cos\theta\right)^2 \left[\Upsilon^4_1 \otimes \int \frac{d^4 l}{(2\pi)^4} \right. \\ &\quad \left. \gamma_L^\mu \left(\frac{i}{m_c \psi + \not{l} - m_s} - \frac{i}{m_c \psi + \not{l} - m_d} \right) \gamma_L^\nu \right]\end{aligned}$$

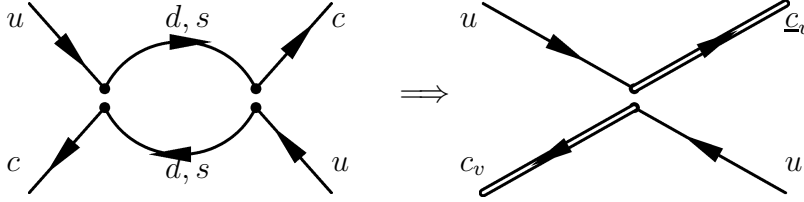


Figure 1: Matching of the four-quark operators at $\mu \approx m_c$

$$\begin{aligned}
& \left[\otimes_D \gamma_{L,\nu} \left(\frac{i}{l - m_s} - \frac{i}{l - m_d} \right) \gamma_{L,\mu} \right] \\
&= -i \frac{1}{\pi^2} \frac{G_F^2}{2} \sin^2 \theta \cos^2 \theta \frac{m_s^4}{m_c^2} \\
& \quad \left[\tau^4_1 \otimes \{ 2 \cdot \gamma_L^\mu \otimes_D \gamma_{L,\mu} + \psi \sigma_L^{\mu\nu} \otimes_D \psi \sigma_{L,\mu\nu} \} \right] \\
&= i \frac{1}{\pi^2} \frac{G_F^2}{2} \sin^2 \theta \cos^2 \theta \frac{m_s^4}{m_c^2} \left[\tau^4_1 \otimes (2\Upsilon^4_1 + 4\Upsilon^4_2) \right]
\end{aligned} \tag{25}$$

to lowest order m_s^2/m_c^2 .

3.3 Six-Quark Operators

For the six-quark operators the color basis is

$$\tau^6_1 = \mathbf{1} \otimes_C \mathbf{1} \otimes_C \mathbf{1} \tag{26}$$

$$\tau^6_2 = T_a \otimes_C T_a \otimes_C \mathbf{1} \tag{27}$$

$$\tau^6_3 = T_a \otimes_C \mathbf{1} \otimes_C T_a \tag{28}$$

$$\tau^6_4 = \mathbf{1} \otimes_C T_a \otimes_C T_a \tag{29}$$

$$\tau^6_5 = d_{abc} \cdot T_a \otimes_C T_b \otimes_C T_c \tag{30}$$

$$\tau^6_6 = f_{abc} \cdot T_a \otimes_C T_b \otimes_C T_c \tag{31}$$

and the basis for the Dirac structure is

$$\Upsilon^6_1 = \gamma_L^\mu \otimes_D \mathbf{1}_L \otimes_D \gamma_{L,\mu} \quad (32)$$

$$\Upsilon^6_2 = \gamma_L^\mu \otimes_D \gamma_{L,\mu} \otimes_D \mathbf{1}_L \quad (33)$$

$$\Upsilon^6_3 = \gamma_L^\mu \otimes_D (\sigma_{L,\mu\nu} \otimes_D \gamma_L^\nu + \gamma_L^\nu \otimes_D \sigma_{L,\mu\nu}) \quad (34)$$

$$\Upsilon^6_4 = \psi_L \otimes_D \gamma_L^\mu \otimes_D \gamma_{L,\mu} \quad (35)$$

$$\Upsilon^6_5 = \psi_L \otimes_D \mathbf{1}_L \otimes_D \mathbf{1}_L. \quad (36)$$

In finding the Dirac basis, we first note that the Dirac piece of the current with two light quarks must contain a γ_L^μ since all light quarks are left-handed. Then we apply the steps discussed in the previous section for the four-quark case. An additional relation

$$\psi \sigma_L^{\kappa\lambda} = i v^\kappa \gamma_L^\lambda - i v^\lambda \gamma_L^\kappa + v_\mu \varepsilon^{\mu\kappa\lambda\nu} \gamma_{L,\nu} \quad (37)$$

allows us to trade contractions of v , ε , and γ_L for σ_L and vice versa. It also allows us to remove the antisymmetric counterpart of Υ^6_3 from the basis.

Now let us consider the matching at the charm mass scale. From the first graph in figure 2 we obtain

$$\begin{aligned} & \left(-i4 \frac{G_F}{\sqrt{2}} \right)^2 \cos \theta \sin \theta (\vec{\kappa} \cdot \vec{\tau}) \left[\tau^6_1 \otimes \left\{ \gamma_{L,\nu} \otimes_D \gamma_{L,\mu} \right. \right. \\ & \left. \left. \otimes_D \left(\gamma_L^\nu \frac{i}{m_c \not{\psi} - m_s} \gamma_L^\mu - \gamma_L^\nu \frac{i}{m_c \not{\psi} - m_d} \gamma_L^\mu \right) \right\} \right]. \quad (38) \end{aligned}$$

Here the matrix $(\vec{\kappa} \cdot \vec{\tau})$ acts on the flavor doublets ψ of down-type quarks appearing in the six-quark operator (see e.g. equation 4)

$$(\vec{\kappa} \cdot \vec{\tau})^{ij} (\bar{\psi}^i u) (\bar{c}_v \psi^j) (\bar{c}_v u).$$

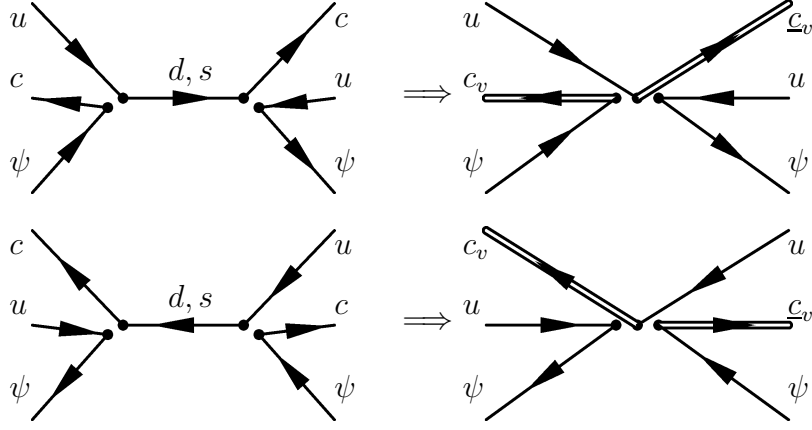


Figure 2: Six-quark matching

where repeated indices are summed. Since $m_d \ll m_s$, (38) reduces to

$$-i 8G_F^2 \cos \theta \sin \theta (\vec{\kappa} \cdot \vec{\tau}) \frac{m_s^2}{m_c^3} \left[\tau^6_1 \otimes \{ \gamma_{L,\nu} \otimes_D \gamma_{L,\mu} \otimes_D \gamma_{L,\nu} \psi \gamma_L^\mu \} \right].$$

Expressing the Dirac structure in terms of our operator basis yields

$$-i 8G_F^2 \cos \theta \sin \theta (\vec{\kappa} \cdot \vec{\tau}) \frac{m_s^2}{m_c^3} \left[\tau^6_1 \otimes \left\{ \frac{1}{2}(\Upsilon^6_1 + \Upsilon^6_2) - i\Upsilon^6_3 - \Upsilon^6_4 \right\} \right]. \quad (39)$$

The second graph in figure 2 also gives a matching contribution of the form (39). In this case, the flavor indices of the matrix $(\vec{\kappa} \cdot \vec{\tau})$ are contracted as follows

$$(\vec{\kappa} \cdot \vec{\tau})^{ij} (\bar{\psi}^i u) (\bar{c}_v u) (\bar{c}_v \psi^j).$$

3.4 Eight-Quark Operators

In studying the color structure for the eight-quark operators, we found it useful to employ a generic $SU(N)$ color group. The number of singlets in

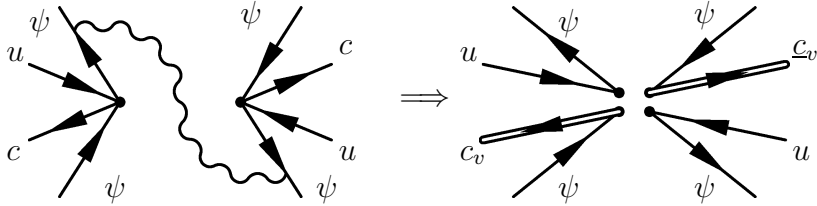


Figure 3: An example of a leading contribution to eight-quark matching.

This graph corresponds to $(l:l::)$ in the notation of section 4.

the tensor product of four adjoint representations of $SU(N)$ is not entirely independent of N : there are 8 singlets for $N = 3$ and 9 for $N > 3$. The difference arises because the rank four tensor

$$d_{abe}d_{cde} + d_{ace}d_{bde} + d_{ade}d_{bce} - \frac{1}{N}\delta_{ab}\delta_{cd} - \frac{1}{N}\delta_{ac}\delta_{bd} - \frac{1}{N}\delta_{ad}\delta_{bc} \quad (40)$$

vanishes [13] for $SU(3)$ and is non-vanishing when $N > 3$. We circumvent this difficulty by constructing a basis with one element proportional to (40). Then the basis for $N = 3$ is the subspace of the $N > 3$ basis that is perpendicular to the (40) direction. The 24 operators for $N > 3$ are listed in appendix A.1.

A straightforward extension of the methods described for the four-quark and six-quark Dirac bases enables us to find the 14 independent eight-quark Dirac structures listed in appendix A.2.

Now we are ready to consider the matching of the eight-quark operators. We have to study graphs similar to the one shown in figure 3 where a gluon is exchanged between two four-fermion operators. Note that not all graphs give a leading (order $\sim 1/m_c^4$) contribution in the effective theory. For instance, graphs in which the gluon couples to two heavy quarks give

operators with coefficients of order $1/m_c^6$: one factor of $1/m_c^2$ comes from each off-shell heavy quark propagator and one more comes from the propagator of the gluon carrying the large momentum of order m_c . Similarly, graphs in which the gluon couples to one heavy and one light quark make contributions of order $(1/m_c^5)$ since an off-shell light quark propagator gives a factor of $(1/m_c)$. The leading graphs are those in which the gluon couples to two light quarks.²

The contribution to the matching made by the graph in figure 3 is

$$8i \frac{G_F^2 4\pi\alpha_s(m_c)}{m_c^4} (\vec{\kappa} \cdot \vec{\tau}) (\vec{\kappa} \cdot \vec{\tau}) \left[\tau_2^8 \otimes \left(-\Upsilon_1^8 - \Upsilon_2^8 + \Upsilon_3^8 + i\Upsilon_5^8 - i\Upsilon_6^8 - \frac{1}{2}\Upsilon_7^8 + \frac{1}{2}\Upsilon_8^8 - \frac{1}{2}\Upsilon_9^8 + \frac{1}{2}\Upsilon_{10}^8 + \frac{i}{2}\Upsilon_{11}^8 - \frac{i}{2}\Upsilon_{12}^8 \right) \right]. \quad (41)$$

Compared to the coefficient of the four-quark operators, (41) has an extra suppression of order α_s/m_c^2 , but no m_s^4 suppression. The matrices $\vec{\kappa} \cdot \vec{\tau}$ act on the flavor indices of the doublets ψ of down-type quarks. Explicitly,

$$(\vec{\kappa} \cdot \vec{\tau})^{ij} (\vec{\kappa} \cdot \vec{\tau})^{kl} (\bar{\psi}^i u) (\bar{\psi}^k u) (\bar{c}_v \psi^j) (\bar{c}_v \psi^l). \quad (42)$$

The contribution from the other graphs is presented in appendix A.3.

4 One-loop integrals

We now compute the one-loop QCD running from m_c to Λ_{QCD} . After discussing the several types of loop integrals occurring in the calculation, we

²Hence the graph in figure 5 of reference [4] is actually subleading.

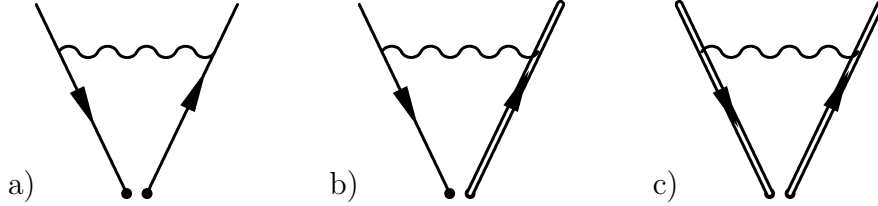


Figure 4: Gluon insertion into light-light, heavy-light, and heavy-heavy pairs of quark lines.

perform the necessary algebra. The calculations for the four-quark operators are easily performed using standard techniques. The eight-quark operator basis is however large enough to make use of symbolic manipulation programs. All our results for the six- and eight-quark operators have been obtained and verified by two independent calculations using the symbolic manipulation tools `Form` [11] and `MathematicaTM` [12]. The algorithm of the `Form` program uses Dirac and $SU(N)$ trace techniques by treating the Dirac algebra as a factor space as discussed in section 3.1. The `Mathematica` program on the other hand implements the reduction from \mathcal{G}_n to $\overline{\mathcal{G}}_n$ explicitly, using relations like (37).

Each loop diagram contributing to the running of our multi-quark operators below the charm scale has one internal gluon and two internal quarks. The form of the loop integral depends on whether the internal quarks are heavy or light. The three possibilities (both heavy, both light, one of each) are sketched in figure 4. Note that each quark line internal to the loop is clearly bounded at one by the gluon insertion and at the other by a vertex connecting it to another quark line. The result of any loop integral may be

expressed simply in terms of the color and Dirac matrices associated with those gluon insertions and vertices. So long as at least one of the internal quarks is heavy, the loop integral turns out to be independent of the Dirac structure of the vertices. For example, (see also appendix B) the integral corresponding to diagram 4b yields

$$I^{hl} = 2 \frac{\alpha}{4\pi} \frac{\mu^\epsilon}{\epsilon} [T_a V_1]^C [T_a V_2]^C + \text{finite} , \quad (43)$$

and that for diagram 4c yields

$$I^{hh} = -4 \frac{\alpha}{4\pi} \frac{\mu^\epsilon}{\epsilon} [T_a V_1]^C [T_a V_2]^C + \text{finite} . \quad (44)$$

Here T_a is the color matrix arising from a gluon insertion and the V_i is the color matrix from the vertex at the other end of the internal quark line. When both internal quarks are light, however, the Dirac structure of the internal quarks' vertices is relevant (fig. 4a)

$$I^{ll} = \frac{1}{2} \frac{\alpha}{4\pi} \frac{\mu^\epsilon}{\epsilon} [T_a V_1]^C [T_a V_2]^C [\gamma^\mu \gamma^\nu V_1]^D [\gamma_\mu \gamma_\nu V_2]^D + \text{finite} . \quad (45)$$

What we have just seen is that the evaluation of each loop diagram falls neatly into three pieces: the momentum integration, the product of color matrices, and the product of Dirac matrices. The first of these is essentially done; we shall address the matrix algebra in the section 5.

We can represent the sum of all 1-loop diagrams renormalizing a $2n$ -quark operator \mathcal{O}_n as a sum over tensor products of linear operators C_i and D_i acting on the color $SU(N)$ and Dirac bases

$$\delta \mathcal{O}_n = \frac{\alpha}{4\pi} \frac{\mu^\epsilon}{\epsilon} \sum_{i=1}^{nD} b_i (C_i \otimes D_i) \mathcal{O}_n \quad (46)$$

where n_D is the number of diagrams. The C_i and D_i come directly from equations 43, 44 and 45. The possible values for the coefficients b_i are $\{\pm 1/2, \pm 2, \pm 4\}$ as we have seen.

Since we will need to evaluate quite a number of one-loop diagrams, it will be useful to have a way of identifying individual diagrams without drawing a picture of each one. As all the one-loop diagrams involved in the running of a particular multi-quark operator differ only in the placement of the single gluon line, this identification is not difficult. For example, recall that we represent a generic four-quark operator by the tensor product (cf. equations (3-5, 6))

$$\Gamma_1 \otimes \Gamma_2.$$

The one-loop diagram in which a gluon is attached to the charm quark and charm anti-quark of this operator could be represented by marking the placement of the gluon insertions

$$G\Gamma_1 \otimes G\Gamma_2.$$

The same information about the placement of the gluon insertions can be conveyed by the briefer notation

$$(l:l)$$

which indicates that the gluon is attached to both the left side of the first current and the left side of the second current. The one-loop diagram in which the gluon is attached to the up quarks would be $(r:r)$ in this notation. The four diagrams in which the gluon is attached to one heavy and one light quark would be represented as $(lr:)$, $(:lr)$, $(l:r)$, and $(r:l)$. The direct correspondence between this ‘colon’ notation and the one-loop diagrams for

the four-quark operators is shown in figure 5. The extension of the notation to the six- and eight-quark operators is straightforward.

Now we can restate our results in colon notation:

- From (3-5) we see that each graph where a gluon connects two heavy lines is of the form $(\dots:l:l)$. For such graphs, $D_i = 1$ and $b_i = 4$.
- The graphs with a light and a heavy quark connected by a gluon also have $D_i = 1$. The coefficient b_i always has magnitude 2. The sign of b_i is positive if the graph is of the form $(\dots r:\dots:l:)$ or $(\dots r:\dots:l)$ and is negative if the graph has the form $(\dots l:\dots:l:)$ or $(\dots l:\dots:l)$.
- The graphs where a gluon connects two light quarks can have a non-trivial Dirac structure. If the graph is of the form $(\dots l:\dots:l\dots)$ or $(\dots r:\dots:r\dots)$ then $D_i \neq 1$ and $b_i = -\frac{1}{2}$. Otherwise, we can apply the following relation for left-handed Dirac matrices Γ_L ³

$$\gamma^\mu \gamma^\nu \gamma_L^\alpha \otimes_D \Gamma_L \gamma_\nu \gamma_\mu = 4 \cdot \gamma_L^\alpha \otimes_D \Gamma_L \quad (47)$$

³From

$$\begin{aligned} & \gamma^\mu \gamma^\nu \gamma_L^\alpha \otimes_D \Gamma_L \gamma_\nu \gamma_\mu - 4 \cdot \gamma_L^\alpha \otimes_D \Gamma_L \\ &= \sigma^{\mu\nu} \gamma_L^\alpha \otimes_D \Gamma_L \sigma_{\mu\nu} = \sigma_R^{\mu\nu} \gamma_L^\alpha \otimes_D \Gamma_L \sigma_{L,\mu\nu} \\ &= (\mathbf{1} \otimes_D \Gamma_L) (\sigma_R^{\mu\nu} \otimes_D \sigma_{L,\mu\nu}) (\gamma_L^\alpha \otimes_D \mathbf{1}) \end{aligned}$$

we see that (47) is a consequence of the identity

$$\sigma_R^{\mu\nu} \otimes_D \sigma_{L,\mu\nu} = 0.$$

to find that $D_i = 1$ and $b_i = 2$.

These observations have interesting consequences in the large N limit. The only diagrams which can give a leading contribution of order αN are those which have a trivial Dirac structure from (47). This can be seen most easily in 't Hooft's double line notation [14], where it is obvious that all diagrams connecting two quark lines on the same side of the operator are not planar and therefore subleading. Therefore the different Dirac structures do not mix in the limit of large N .

5 Anomalous Dimensions

Having calculated the divergent pieces of the loop integrals, we can now proceed to use the renormalization group equation

$$\left(\mu \frac{\partial}{\partial \mu} + \beta(g) \frac{\partial}{\partial g} + n_l \gamma_l + n_h \gamma_h - \gamma_n \right) \mathcal{O}_n = 0 \quad (48)$$

to extract the anomalous dimensions γ_n . Here n_l and n_h are, respectively, the number of heavy and light quark fields in the operator \mathcal{O}_n and $n = n_l + n_h$. Using [9]

$$\beta(g) = -\frac{g_s^3}{16\pi^2} \frac{11N - 2n_f}{3} \quad (49)$$

$$\gamma_l = -C_F \frac{\alpha_s}{4\pi} \quad (50)$$

$$\gamma_h = 2C_F \frac{\alpha_s}{4\pi} \quad (51)$$

with $n_f = 3$ the number of light quark flavors below the charm scale, we arrive at the anomalous dimension matrix

$$\gamma_n = \frac{\alpha_s}{4\pi} \left[\sum_i b_i (C_i \otimes D_i) + (2n_h - n_l) C_F \cdot (\mathbf{1} \otimes \mathbf{1}) \right] + O(\alpha_s^2) \quad (52)$$

where b_i , C_i and D_i have been defined in section 4.

The Wilson coefficients $\eta_i(\mu)$ in the effective Hamiltonian

$$H_{eff} = G_F^2 \sum_i \eta_i(\mu) O_i(\mu) \quad (53)$$

satisfy the renormalization group equation

$$\mu \frac{d}{d\mu} \eta_i(\mu) = -(\gamma_n)_{ij}^T \eta_j(\mu), \quad (54)$$

where γ_n^T is the transpose of the anomalous dimension matrix from (48). If we decompose γ_n^T as

$$\gamma_n^T = L_n \cdot \gamma_n^D \cdot R_n, \quad L = R^{-1} \quad (55)$$

with γ_n^D a diagonal matrix and expand γ_n^D in powers of α_s ,

$$\gamma_n^D = \frac{\alpha_s}{4\pi} \tilde{\gamma}_n^D + O(\alpha_s^2). \quad (56)$$

the solution of (54) may be expressed in the form

$$\eta(\mu) = L_n \cdot \left(\frac{\alpha_s(\mu)}{\alpha_s(m_c)} \right)^{\frac{3\tilde{\gamma}_n^D}{2(11N - 2n_f)}} \cdot R_n \cdot \eta(m_c). \quad (57)$$

In QCD with three light quark flavors below m_c , the exponent of (57) simplifies to $\tilde{\gamma}_n^D/18$. Since α_s increases as we run down from the charm scale, a positive exponent $\tilde{\gamma}_n^D$ will result in enhancement of the coefficient η .

In the rest of this section, we will calculate the anomalous dimensions of the multi-quark operators responsible for D^0 - \bar{D}^0 mixing. We will use these anomalous dimensions to run our Wilson coefficients to a hadronic scale of order Λ_{QCD} in the next section.

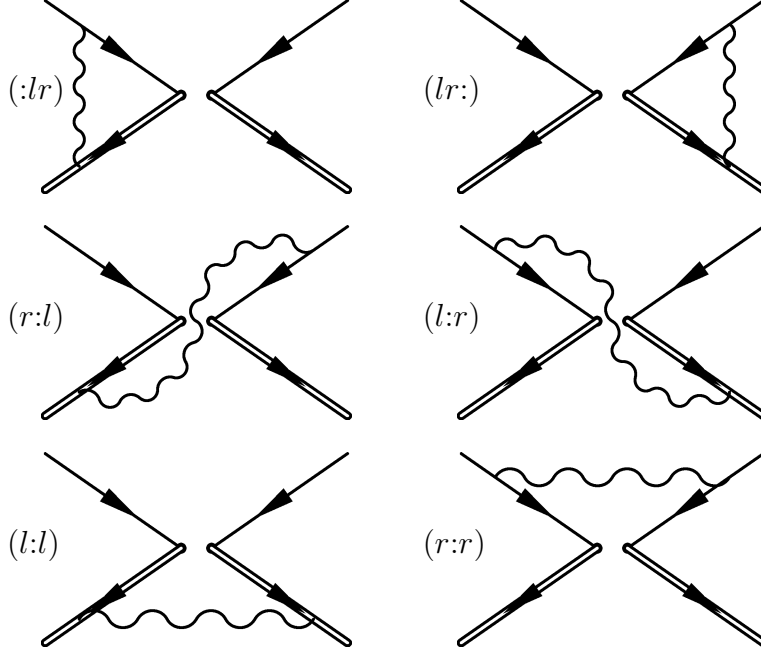


Figure 5: Running of the four-quark operators

5.1 Four-Quark Operators

The Feynman diagrams contributing to the running of the four-quark operators below m_c are shown in fig. 5. Using the rules and the notation explained in section 4 we can immediately infer

$$D_{(:lr)} = D_{(lr:)} = D_{(r:l)} = D_{(l:r)} = D_{(l:l)} = \mathbf{1} \quad (58)$$

and

$$b_{(:lr)} = b_{(lr:)} = b_{(r:l)} = b_{(l:r)} = 2, \quad b_{(l:l)} = 4, \quad b_{(r:r)} = -\frac{1}{2}. \quad (59)$$

A short calculation yields for the color structure

$$C_{(:lr)} = C_{(lr:)} = \begin{pmatrix} C_F & 0 \\ 0 & -\frac{1}{2N} \end{pmatrix} \quad (60)$$

$$C_{(r:l)} = C_{(l:r)} = \begin{pmatrix} 0 & 1 \\ \frac{C_F}{2N} & C_F - \frac{1}{2N} \end{pmatrix} \quad (61)$$

$$C_{(l:l)} = C_{(r:r)} = \begin{pmatrix} 0 & 1 \\ \frac{C_F}{2N} & -\frac{1}{N} \end{pmatrix} \quad (62)$$

and for the remaining Dirac structure

$$D_{(r:r)} = \begin{pmatrix} 16 & 0 \\ -4 & 0 \end{pmatrix}. \quad (63)$$

Using the general relation (52), the anomalous dimensions for the four-quark operators read explicitly

$$(\gamma_4)^T = \frac{\alpha_s}{4\pi} \left\{ \begin{pmatrix} 6C_F & \frac{4C_F}{N} \\ 8 & 6C_F - \frac{8}{N} \end{pmatrix} \otimes \mathbf{1} + \begin{pmatrix} 0 & -\frac{C_F}{4N} \\ -\frac{1}{2} & \frac{1}{2N} \end{pmatrix} \otimes D_{(r:r)}^T \right\}. \quad (64)$$

The first term in the sum (64) takes into account the contributions of graphs $(:lr)$, $(lr:)$, $(r:l)$, $(l:r)$, $(l:l)$, and the self energy subtraction. The second term in (64) is the contribution of the last graph $(r:r)$.

The simple form of (64) allows us to perform the decomposition (55) separately for the color and the Dirac part:

$$\tilde{\gamma}_4 = 6C_F \cdot \mathbf{1} \otimes \mathbf{1} + 4 \cdot \begin{pmatrix} 1 - \frac{1}{N} & 0 \\ 0 & -1 - \frac{1}{N} \end{pmatrix} \otimes \begin{pmatrix} 0 & 0 \\ 0 & 1 \end{pmatrix} \quad (65)$$

$$L_4 = \begin{pmatrix} 1 + \frac{1}{N} & 1 - \frac{1}{N} \\ 2 & -2 \end{pmatrix} \otimes \begin{pmatrix} 1 & 1 \\ 0 & 4 \end{pmatrix} \quad (66)$$

$$R_4 = \begin{pmatrix} \frac{1}{2} & \frac{N-1}{4N} \\ \frac{1}{2} & -\frac{N+1}{4N} \end{pmatrix} \otimes \begin{pmatrix} 1 & -\frac{1}{4} \\ 0 & \frac{1}{4} \end{pmatrix} \quad (67)$$

and we can read off the eigenvalues from (65)

$$\frac{\alpha}{\pi} \left(\frac{3}{2} C_F - 1 - \frac{1}{N} \right), \quad \frac{\alpha}{\pi} \left(\frac{3}{2} C_F + 1 - \frac{1}{N} \right), \quad \frac{\alpha}{\pi} \frac{3}{2} C_F, \quad \frac{\alpha}{\pi} \frac{3}{2} C_F, \quad (68)$$

corresponding to the exponents $16/27$, $4/27$, $4/9$, and $4/9$ in 57.

5.2 Six-Quark Operators

The simple structure of our results for the four-quark operators does not persist in the six-quark case. The gluon insertions with non trivial action on the Dirac basis (32-36) are

$$D_{(:r:r)} = \begin{pmatrix} 2 & 2 & -2i & 4 & 0 \\ 2 & 2 & -2i & -4 & 0 \\ 12i & 12i & 12 & 0 & 0 \\ 0 & 0 & 0 & 16 & 0 \\ 0 & 0 & 0 & -4 & 0 \end{pmatrix} \quad (69)$$

$$D_{(r:r)} = \begin{pmatrix} 6 & -2 & 2i & -4 & 0 \\ 0 & 16 & 0 & 0 & 0 \\ -18i & 6i & 6 & 12i & 0 \\ -6 & -6 & -2i & 4 & 0 \\ 0 & 4 & 0 & 0 & 0 \end{pmatrix} \quad (70)$$

$$D_{(r::r)} = \begin{pmatrix} 16 & 0 & 0 & 0 & 0 \\ -2 & 6 & 2i & 4 & 0 \\ 6i & -18i & 6 & -12i & 0 \\ 6 & 6 & 2i & 4 & 0 \\ -4 & 0 & 0 & 0 & 0 \end{pmatrix}. \quad (71)$$

While each matrix has the same set of eigenvalues $(16, 16, 0, 0, 0)$, the corresponding eigenspaces differ and the diagonalization method of the preceding section is not applicable. We can nevertheless pick a particular value for N ($N = 3$ being the natural choice) and perform the decomposition (55) of γ_6^T numerically. In this way we obtain the multiplicities for the exponents shown in figure 6. The two largest exponents are $17/18$, resulting in an appreciable enhancement of the related operators.

5.3 Eight-Quark Operators

In the case of the eight-quark operators, there are seven non-trivial 14-dimensional matrices describing the 1-loop mixing of the Dirac space operators. Rather than quoting those here, we proceed immediately to an account of the numerical results. In figure 7 we have plotted the multiplicities of the exponents of the anomalous dimension matrix $\tilde{\gamma}_8^D/18$ for the eight-quark operators for $N = 3$.

The largest exponents are $37/27$ and $11/9$ with multiplicities 2 and 5, respectively. Over all, eighteen operator coefficients have exponents greater than or equal to 1; for these operator coefficients, the QCD running effectively removes the suppression factor of $\alpha_s(m_c)$ introduced in the charm-scale

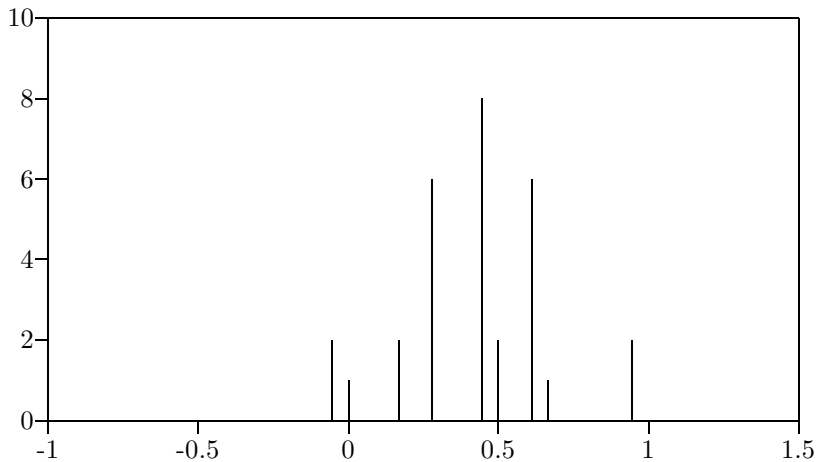


Figure 6: Multiplicity distribution of the eigenvalues of the anomalous dimension matrix $\tilde{\gamma}_8^D/18$ for the six-quark operators in the case $N = 3$.

matching.

6 Matrix Elements

We can now run our Wilson coefficients all the way down to a typical hadronic scale where it is possible to evaluate the matrix elements contributing to the D -meson mass difference:

$$\Delta m = 2 \cdot \langle D^0 | H_{eff} | \bar{D}^0 \rangle. \quad (72)$$

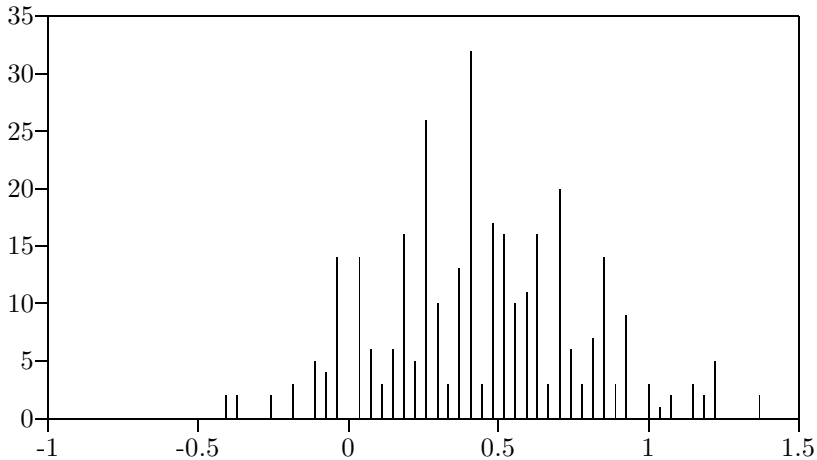


Figure 7: Multiplicity distribution of the eigenvalues of the anomalous dimension matrix $\tilde{\gamma}_8^D/18$ for the eight-quark operators in the case $N = 3$.

In principle, the evaluation of these matrix elements requires non-perturbative methods, e.g. lattice gauge theory calculations. Instead, we will estimate the size of the matrix elements using Naive Dimensional Analysis (NDA) [10, 4].

Throughout this paper, we have abbreviated our multi-quark operators by writing down tensor-products of color and Dirac matrices without the accompanying quark fields. Now that we are about to calculate matrix elements, we remind the reader that the operators τ_i^{2n} and Υ_i^{2n} do really

carry quark fields with them. For example, where we write

$$(\vec{\kappa} \cdot \vec{\tau}) \tau_2^6 \otimes \Upsilon_1^6$$

we mean

$$(\kappa \cdot \tau)^{mn} \left(\bar{\psi}^m [T_a \otimes \gamma_L^\mu] u \right) (\bar{c}_v [T_a \otimes \mathbf{1}] \psi^n) (\bar{c}_v [\mathbf{1} \otimes \gamma_{L,\mu}] u).$$

We will continue to use this convention in order to keep the expressions for the matrix elements relatively compact.

The contribution of the four-quark operators to the D -meson mass difference is given by the results of our matching (25) and running (57) calculations as

$$(\Delta m)_4 = 4 \times 2 \cdot \frac{1}{16\pi^2} G_F^2 \sin^2 \theta \cos^2 \theta \frac{m_s^4}{m_c^2} \times \sum_{i,j=1,2} \eta_{ij}^4(\Lambda) \langle D^0 | 4\tau_i^4 \Upsilon_j^4 | \bar{D}^0 \rangle, \quad (73)$$

where Λ is a typical hadronic scale which we fix by the condition $\alpha_s(\Lambda) = 1$. Note that the factor of 4 in the $4\Upsilon_j^4$ confers a conventional normalization on the Dirac operators (i.e. multiplies each left-handed projection operator by a factor of two). The initial conditions at the charm scale may be read from (25)

$$\eta_{11}^4(m_c) = 1 \quad (74)$$

$$\eta_{12}^4(m_c) = 2 \quad (75)$$

$$\eta_{21}^4(m_c) = \eta_{22}^4(m_c) = 0 \quad (76)$$

Using the values [15]

$$\cos \theta = 0.975 \quad (77)$$

$$G_F = 1.166 \cdot 10^{-5} \text{ GeV}^{-2} \quad (78)$$

$$m_c = 1.5 \text{ GeV}, \quad (79)$$

we find

$$(\Delta m)_4 = 23 \times 10^{-17} \text{ GeV}^{-2} \left(\frac{m_s}{0.2 \text{ GeV}} \right)^4 \times \sum_{i,j=1,2} \eta_{ij}^4(\Lambda) \langle D^0 | 4\tau^4_i \Upsilon^4_j | \bar{D}^0 \rangle. \quad (80)$$

We must now estimate the magnitude of the hadronic matrix elements. NDA tells us

$$\langle D^0 | 4\tau^4_i \Upsilon^4_j | \bar{D}^0 \rangle \approx m_c f_D^2 \approx \Lambda_{\chi SB} f^2 \approx \frac{1}{16\pi^2} \Lambda_{\chi SB}^3 \quad (81)$$

where $\Lambda_{\chi SB} \approx 1 \text{ GeV}$ is the chiral symmetry breaking scale. Note that NDA does not tell us whether the matrix elements of our several operators will interfere constructively or destructively. In the context of dimensional analysis, it is not unreasonable to assume statistical independence of the various contributions and to add the coefficients in quadrature. We can also obtain a reasonable upper estimate by adding the magnitudes of the individual contributions.

Using these two procedures as limiting cases, the result without the leading order QCD corrections is

$$(\Delta m)_4^0 \approx (0.3 - 0.4) \cdot 10^{-17} \text{ GeV} \left(\frac{m_s}{0.2 \text{ GeV}} \right)^4,$$

in agreement with the result for the short distance contribution from the box diagram. Using

$$\alpha_s(m_c) = 0.4 \quad (82)$$

the renormalization group running enhances this to

$$(\Delta m)_4 \approx (0.5 - 0.9) \cdot 10^{-17} \text{ GeV} \left(\frac{m_s}{0.2 \text{ GeV}} \right)^4. \quad (83)$$

To evaluate the contribution of the six-quark operators to the mass difference, we follow a similar line of reasoning. Since NDA suggests that the matrix element of the U -spin vector operator $\bar{\psi} \vec{\kappa} \cdot \vec{\tau} \psi$ is of the order $\sin \theta \cos \theta m_s f^2$ [4], we expect the matrix elements of the six-quark operators to yield

$$\langle D^0 | 8(\vec{\kappa} \cdot \vec{\tau}) \tau_i^6 \Upsilon_j^6 | \bar{D}^0 \rangle \approx (\sin \theta \cos \theta m_s f^2) (m_c f_D^2). \quad (84)$$

Combining this estimate with our results from the matching (38) and running (57) calculations (keeping in mind that two distinct diagrams contribute to the matching) yields

$$\begin{aligned} (\Delta m)_6 &= 2 \cdot \frac{1}{2} \frac{\Lambda_{\chi SB}^2}{m_s m_c} \times 2 \cdot \frac{1}{16\pi^2} G_F^2 \sin^2 \theta \cos^2 \theta \frac{m_s^4}{m_c^2} \times \\ &\quad \frac{1}{\sin \theta \cos \theta m_s f^2} \sum_{i,j} \eta_{ij}^6(\Lambda) \langle D^0 | (\vec{\kappa} \cdot \vec{\tau}) 8\tau_i^6 \Upsilon_j^6 | \bar{D}^0 \rangle. \end{aligned} \quad (85)$$

Then we find

$$(\Delta m)_6^0 \approx (0.4 - 0.7) \cdot 10^{-17} \text{ GeV} \left(\frac{m_s}{0.2 \text{ GeV}} \right)^3$$

from the charm-quark matching and

$$(\Delta m)_6 \approx (0.7 - 2.0) \cdot 10^{-17} \text{ GeV} \left(\frac{m_s}{0.2 \text{ GeV}} \right)^3 \quad (86)$$

including the leading order QCD corrections

Repeating this reasoning for the eight-quark operators, we have

$$\langle D^0 | (\vec{\kappa} \cdot \vec{\tau})^2 16\tau_i^8 \Upsilon_j^8 | \bar{D}^0 \rangle \approx (\sin \theta \cos \theta m_s f^2)^2 (m_c f_D^2) \quad (87)$$

and applying this to (41) and (57) gives

$$\begin{aligned}
(\Delta m)_8 &= \frac{1}{4} \frac{\alpha(m_c)}{4\pi} \frac{\Lambda_{\chi SB}^4}{m_s^2 m_c^2} \times 2 \cdot \frac{1}{16\pi^2} G_F^2 \sin^2 \theta \cos^2 \theta \frac{m_s^4}{m_c^2} \times \\
&\quad \left(\frac{1}{\sin \theta \cos \theta m_s f^2} \right)^2 \sum_{i,j} \eta_{ij}^8(\Lambda) \langle D^0 | (\vec{\kappa} \cdot \vec{\tau})^2 16\tau_i^8 \Upsilon_j^8 | \bar{D}^0 \rangle.
\end{aligned} \tag{88}$$

The charm-scale matching gives

$$(\Delta m)_8^0 \approx (0.04 - 0.2) \cdot 10^{-17} \text{ GeV} \left(\frac{m_s}{0.2 \text{ GeV}} \right)^2$$

and the numerical solution of the renormalization group equation yields

$$(\Delta m)_8 \approx (0.07 - 0.6) \cdot 10^{-17} \text{ GeV} \left(\frac{m_s}{0.2 \text{ GeV}} \right)^2. \tag{89}$$

The large number of contributing operators causes a substantial uncertainty in the last expression because our estimate of the error from the unknown phases scales roughly like $\sqrt{\text{number of operators}}$. This uncertainty does not, however, apply to the upper bound.

Adding all contributions, our final result is

$$(\Delta m)_{HqEFT} \approx (0.9 - 3.5) \cdot 10^{-17} \text{ GeV} \tag{90}$$

for $m_s = 0.2 \text{ GeV}$.

7 Conclusions

We have calculated the leading order QCD corrections to D^0 - \bar{D}^0 mixing in the Heavy Quark Effective Field Theory. We find that the renormalization group running enhances Δm by a factor of two to three. While the precision of our

numerical results is limited by our incomplete knowledge of the hadronic matrix elements, we do *not* see any large correction to the purely short distance contribution in the framework of HqEFT. We therefore conclude that the cancellations among the dispersive channels conjectured in [4] are not removed by the leading order QCD corrections.

Acknowledgements

We are grateful to Howard Georgi for stimulating our interest by sharing his unconventional views on the subject and for comments on the manuscript. Mike Dugan provided us with valuable group theoretical suggestions. This research has been supported in part by the National Science Foundation under Grant #PHY-8714654 and by the Texas National Research Laboratory Commission under grant RGFY9206. T. O. acknowledges financial support from Deutsche Forschungsgemeinschaft (Germany) under Grant # Oh 56/1-1. G. R. acknowledges financial support from INFN (Italy).

References

- [1] M. K. Gaillard and B. W. Lee, Phys. Rev. **D10** (1974) 897.
- [2] H. Georgi, *Physics from Vacuum Alignment in A Technicolor Model*, Preprint HUTP-92/A037.
- [3] C. D. Carone, R. T. Hamilton, *Flavor Changing Neutral Currents in a Realistic Composite Technicolor Model*, Preprint HUTP-92/A059.

- [4] H. Georgi, *D- \bar{D} Mixing in Heavy Quark Effective Field Theory*, Preprint HUTP-92/A049, hep-ph/9209291.
- [5] L. Wolfenstein, Phys. Lett. **164B** (1985) 170.
- [6] J. F. Donoghue, E. Golowich, B. R. Holstein, and J. Trampetić, Phys. Rev. **D33** (1986) 179.
- [7] J. F. Donoghue, E. Golowich and B. R. Holstein, Phys. Lett. **135B** (1984) 481.
- [8] N. Isgur and M. B. Wise, Phys. Lett. **208B** (1988) 504; **232 B** (1989) 113. E. Eichten and B. Hill, Phys. Lett. **234B** (1990) 511. B. Grinstein, Nucl. Phys. **B339** (1990) 253. H. Georgi, Phys. Lett. **B240** (1990) 447.
- [9] H. Georgi, *Heavy Quark Effective Field Theory*, in: Proc. of the Theoretical Advanced Study Institute 1991, eds. R. K. Ellis, C.T. Hill, and J.D. Lykken (World Scientific, Singapore, 1992) p. 589.
- [10] S. Weinberg, Physica **96A** (1979) 327. A. Manohar and H. Georgi, Nucl. Phys. **B234** (1984) 189. H. Georgi and L. Randall, Nucl. Phys. **B276** (1986) 241.
- [11] J. A. M. Vermaseren, *Symbolic Manipulation with FORM*, Amsterdam, 1991.
- [12] S. Wolfram, *MathematicaTM*, Reading, MA, 1991.
- [13] A. J. Macfarlane, A. Sudbery and P. H. Weisz, Comm. math. Phys. **11** (1968) 77.

[14] G. 't Hooft, Nucl. Phys. **B72** (1974) 461.

[15] Particle Data Group, *Review of Particle Properties*, Phys. Rev. **D45** Part 2. (1992).

A Eight-Quark Operator Basis

A.1 Color Structure

Let us fix the notation for the invariant tensors f and d

$$f_{abc} = -2i \text{Tr} ([T_a, T_b] T_c) \quad (91)$$

$$d_{abc} = 2 \text{Tr} (\{T_a, T_b\} T_c). \quad (92)$$

Then the color basis for the eight-quark operators is

$$\tau_1^8 = \mathbf{1} \otimes_C \mathbf{1} \otimes_C \mathbf{1} \otimes_C \mathbf{1} \quad (93)$$

$$\tau_2^8 = T_a \otimes_C T_a \otimes_C \mathbf{1} \otimes_C \mathbf{1} \quad (94)$$

$$\tau_3^8 = \mathbf{1} \otimes_C \mathbf{1} \otimes_C T_a \otimes_C T_a \quad (95)$$

$$\tau_4^8 = T_a \otimes_C \mathbf{1} \otimes_C T_a \otimes_C \mathbf{1} \quad (96)$$

$$\tau_5^8 = \mathbf{1} \otimes_C T_a \otimes_C \mathbf{1} \otimes_C T_a \quad (97)$$

$$\tau_6^8 = T_a \otimes_C \mathbf{1} \otimes_C \mathbf{1} \otimes_C T_a \quad (98)$$

$$\tau_7^8 = \mathbf{1} \otimes_C T_a \otimes_C T_a \otimes_C \mathbf{1} \quad (99)$$

$$\tau_8^8 = f_{abc} \cdot T_a \otimes_C T_b \otimes_C T_c \otimes_C \mathbf{1} \quad (100)$$

$$\tau_9^8 = d_{abc} \cdot T_a \otimes_C T_b \otimes_C T_c \otimes_C \mathbf{1} \quad (101)$$

$$\tau_{10}^8 = f_{abc} \cdot T_a \otimes_C T_b \otimes_C \mathbf{1} \otimes_C T_c \quad (102)$$

$$\tau_{11}^8 = d_{abc} \cdot T_a \otimes_C T_b \otimes_C \mathbf{1} \otimes_C T_c \quad (103)$$

$$\tau_{12}^8 = f_{abc} \cdot T_a \otimes_C \mathbf{1} \otimes_C T_b \otimes_C T_c \quad (104)$$

$$\tau_{13}^8 = d_{abc} \cdot T_a \otimes_C \mathbf{1} \otimes_C T_b \otimes_C T_c \quad (105)$$

$$\tau_{14}^8 = f_{abc} \cdot \mathbf{1} \otimes_C T_a \otimes_C T_b \otimes_C T_c \quad (106)$$

$$\tau_{15}^8 = d_{abc} \cdot \mathbf{1} \otimes_C T_a \otimes_C T_b \otimes_C T_c \quad (107)$$

$$\tau_{16}^8 = \delta_{ab}\delta_{cd} \cdot T_a \otimes_C T_b \otimes_C T_c \otimes_C T_d \quad (108)$$

$$\tau_{17}^8 = d_{abe}d_{cde} \cdot T_a \otimes_C T_b \otimes_C T_c \otimes_C T_d \quad (109)$$

$$\tau_{18}^8 = f_{abe}d_{cde} \cdot T_a \otimes_C T_b \otimes_C T_c \otimes_C T_d \quad (110)$$

$$\tau_{19}^8 = d_{abe}f_{cde} \cdot T_a \otimes_C T_b \otimes_C T_c \otimes_C T_d \quad (111)$$

$$\tau_{20}^8 = f_{abe}f_{cde} \cdot T_a \otimes_C T_b \otimes_C T_c \otimes_C T_d \quad (112)$$

$$\begin{aligned} \tau_{21}^8 = & (f_{ace}d_{bde} - f_{ade}d_{bce} - f_{bce}d_{ade} + f_{bde}d_{ace}) \\ & \cdot T_a \otimes_C T_b \otimes_C T_c \otimes_C T_d \end{aligned} \quad (113)$$

$$\tau_{22}^8 = (\delta_{ac}\delta_{bd} - \delta_{ad}\delta_{bc}) \cdot T_a \otimes_C T_b \otimes_C T_c \otimes_C T_d \quad (114)$$

$$\tau_{23}^8 = (\delta_{ac}\delta_{bd} + \delta_{ad}\delta_{bc}) \cdot T_a \otimes_C T_b \otimes_C T_c \otimes_C T_d \quad (115)$$

$$\begin{aligned} \tau_{24}^8 = & \left(d_{abe}d_{cde} + d_{ace}d_{bde} + d_{ade}d_{bce} \right. \\ & \left. - \frac{1}{N} (\delta_{ab}\delta_{cd} + \delta_{ac}\delta_{bd} + \delta_{ad}\delta_{bc}) \right) \cdot T_a \otimes_C T_b \otimes_C T_c \otimes_C T_d \end{aligned} \quad (116)$$

A.2 Dirac structures

Our basis for the Dirac structure of the eight-quark operators is

$$\Upsilon_1^8 = \gamma_L^\mu \otimes_D \gamma_{L,\mu} \otimes_D \gamma_L^\nu \otimes_D \gamma_{L,\nu} \quad (117)$$

$$\Upsilon_2^8 = \gamma_L^\mu \otimes_D \gamma_L^\nu \otimes_D \gamma_{L,\mu} \otimes_D \gamma_{L,\nu} \quad (118)$$

$$\Upsilon_3^8 = \gamma_L^\mu \otimes_D \gamma_L^\nu \otimes_D \gamma_{L,\nu} \otimes_D \gamma_{L,\mu} \quad (119)$$

$$\Upsilon^8_4 = \gamma_L^\mu \otimes_D \gamma_{L,\mu} \otimes_D \mathbf{1}_L \otimes_D \mathbf{1}_L \quad (120)$$

$$\Upsilon^8_5 = \gamma_L^\mu \otimes_D \gamma_L^\nu \otimes_D \sigma_{L,\mu\nu} \otimes_D \mathbf{1}_L \quad (121)$$

$$\Upsilon^8_6 = \gamma_L^\mu \otimes_D \gamma_L^\nu \otimes_D \mathbf{1}_L \otimes_D \sigma_{L,\mu\nu} \quad (122)$$

$$\Upsilon^8_7 = \gamma_L^\mu \otimes_D \psi_L \otimes_D \gamma_{L,\mu} \otimes_D \mathbf{1}_L \quad (123)$$

$$\Upsilon^8_8 = \psi_L \otimes_D \gamma_L^\mu \otimes_D \gamma_{L,\mu} \otimes_D \mathbf{1}_L \quad (124)$$

$$\Upsilon^8_9 = \gamma_L^\mu \otimes_D \psi_L \otimes_D \mathbf{1}_L \otimes_D \gamma_{L,\mu} \quad (125)$$

$$\Upsilon^8_{10} = \psi_L \otimes_D \gamma_L^\mu \otimes_D \mathbf{1}_L \otimes_D \gamma_{L,\mu} \quad (126)$$

$$\Upsilon^8_{11} = \gamma_L^\mu \otimes_D \psi_L \otimes_D (\gamma_L^\nu \otimes_D \sigma_{L,\mu\nu} + \sigma_{L,\mu\nu} \otimes_D \gamma_L^\nu) \quad (127)$$

$$\Upsilon^8_{12} = \psi_L \otimes_D \gamma_L^\mu \otimes_D (\gamma_L^\nu \otimes_D \sigma_{L,\mu\nu} + \sigma_{L,\mu\nu} \otimes_D \gamma_L^\nu) \quad (128)$$

$$\Upsilon^8_{13} = \psi_L \otimes_D \psi_L \otimes_D \gamma_L^\mu \otimes_D \gamma_{L,\mu} \quad (129)$$

$$\Upsilon^8_{14} = \psi_L \otimes_D \psi_L \otimes_D \mathbf{1}_L \otimes_D \mathbf{1}_L \quad (130)$$

Note that potential contributions proportional to $\varepsilon^{\alpha\beta\gamma\delta} \gamma_{L,\alpha} \otimes_D \gamma_{L,\beta} \otimes_D \gamma_{L,\gamma} \otimes_D \gamma_{L,\delta}$ have been eliminated, because the identity⁴

$$\forall v^2 > 0 : v^2 \varepsilon^{\alpha\beta\gamma\delta} = v^\alpha v_\mu \varepsilon^{\mu\beta\gamma\delta} + v^\beta v_\mu \varepsilon^{\mu\alpha\gamma\delta} + v^\gamma v_\mu \varepsilon^{\mu\alpha\beta\delta} + v^\delta v_\mu \varepsilon^{\mu\alpha\beta\gamma} \quad (131)$$

can be used to relate them to elements of the basis.

A.3 Matching

In this appendix we give the results of the leading order matching for each graph in terms of the basis listed in appendix A. To distinguish the individual

⁴In a system of coordinate with $v = (\sqrt{v^2}, \vec{0})$ equation (131) is nothing but the familiar expansion formula for a determinant in terms of its minors.

graphs, we use the notation introduced at the end of section 4. All the following terms have the overall factor

$$8i \frac{G_F^2 4\pi\alpha_s(m_c)}{m_c^4} (\vec{k} \cdot \vec{\tau})(\vec{k} \cdot \vec{\tau}) \quad (132)$$

where α_s is the strong coupling and the two matrices $\vec{k} \cdot \vec{\tau}$ are intended to act over the doublets ψ , as explained in section 3.4

$$\begin{aligned} (::r:r) \mapsto & \tau^8_3 \otimes \left(-\Upsilon^8_1 - \Upsilon^8_2 + \Upsilon^8_3 - i\Upsilon^8_5 + i\Upsilon^8_6 + \frac{1}{2}\Upsilon^8_7 \right. \\ & \left. - \frac{1}{2}\Upsilon^8_8 + \frac{1}{2}\Upsilon^8_9 - \frac{1}{2}\Upsilon^8_{10} - \frac{i}{2}\Upsilon^8_{11} + \frac{i}{2}\Upsilon^8_{12} \right) \end{aligned} \quad (133)$$

$$\begin{aligned} (r:::r) \mapsto & \tau^8_6 \otimes \left(+\Upsilon^8_1 - \Upsilon^8_2 - \Upsilon^8_3 + i\Upsilon^8_5 - i\Upsilon^8_6 - \frac{1}{2}\Upsilon^8_7 \right. \\ & \left. + \frac{1}{2}\Upsilon^8_8 - \frac{1}{2}\Upsilon^8_9 + \frac{1}{2}\Upsilon^8_{10} + \frac{i}{2}\Upsilon^8_{11} - \frac{i}{2}\Upsilon^8_{12} \right) \end{aligned} \quad (134)$$

$$\begin{aligned} (r:l::) \mapsto & \tau^8_2 \otimes \left(-\Upsilon^8_1 + \Upsilon^8_2 + \Upsilon^8_3 - 2\Upsilon^8_4 + i\Upsilon^8_5 + i\Upsilon^8_6 - \frac{1}{2}\Upsilon^8_7 \right. \\ & \left. + \frac{7}{2}\Upsilon^8_8 - \frac{1}{2}\Upsilon^8_9 - \frac{1}{2}\Upsilon^8_{10} + \frac{i}{2}\Upsilon^8_{11} + \frac{i}{2}\Upsilon^8_{12} + 2\Upsilon^8_{13} \right) \end{aligned} \quad (135)$$

$$\begin{aligned} (l:r::) \mapsto & \tau^8_2 \otimes \left(-\Upsilon^8_1 + \Upsilon^8_2 + \Upsilon^8_3 - 2\Upsilon^8_4 - i\Upsilon^8_5 - i\Upsilon^8_6 + \frac{1}{2}\Upsilon^8_7 \right. \\ & \left. + \frac{1}{2}\Upsilon^8_8 - \frac{7}{2}\Upsilon^8_9 + \frac{1}{2}\Upsilon^8_{10} - \frac{i}{2}\Upsilon^8_{11} - \frac{i}{2}\Upsilon^8_{12} + 2\Upsilon^8_{13} \right) \end{aligned} \quad (136)$$

$$\begin{aligned} (:l:r:) \mapsto & \tau^8_7 \otimes \left(\Upsilon^8_1 + \Upsilon^8_2 - \Upsilon^8_3 + 2\Upsilon^8_4 - i\Upsilon^8_5 - i\Upsilon^8_6 + \frac{1}{2}\Upsilon^8_7 \right. \\ & \left. - \frac{7}{2}\Upsilon^8_8 + \frac{1}{2}\Upsilon^8_9 + \frac{1}{2}\Upsilon^8_{10} - \frac{i}{2}\Upsilon^8_{11} - \frac{i}{2}\Upsilon^8_{12} - 2\Upsilon^8_{13} \right) \end{aligned} \quad (137)$$

$$\begin{aligned} (l:::r) \mapsto & \tau^8_6 \otimes \left(\Upsilon^8_1 + \Upsilon^8_2 - \Upsilon^8_3 + 2\Upsilon^8_4 + i\Upsilon^8_5 + i\Upsilon^8_6 - \frac{1}{2}\Upsilon^8_7 \right. \\ & \left. - \frac{1}{2}\Upsilon^8_8 + \frac{7}{2}\Upsilon^8_9 - \frac{1}{2}\Upsilon^8_{10} + \frac{i}{2}\Upsilon^8_{11} + \frac{i}{2}\Upsilon^8_{12} - 2\Upsilon^8_{13} \right) \end{aligned} \quad (138)$$

$$\begin{aligned} (l:l::) \mapsto & \tau^8_2 \otimes \left(-\Upsilon^8_1 - \Upsilon^8_2 + \Upsilon^8_3 + i\Upsilon^8_5 - i\Upsilon^8_6 - \frac{1}{2}\Upsilon^8_7 \right. \\ & \left. + \frac{1}{2}\Upsilon^8_8 - \frac{1}{2}\Upsilon^8_9 + \frac{1}{2}\Upsilon^8_{10} + \frac{i}{2}\Upsilon^8_{11} - \frac{i}{2}\Upsilon^8_{12} \right) \end{aligned} \quad (139)$$

Two additional graphs are connected to the preceding by symmetry; the graph $(:r:r:)$ is the same as $(r:::r)$ but with a different color factor τ^8_7 and $(r:r::)$ is the same as $(::r:r)$ but with a color factor τ^8_2 .

B One-Loop Integrals

Using the one-loop integrals

$$\mu^\epsilon \int \frac{d^{4-\epsilon}l}{(2\pi)^{4-\epsilon}} \frac{l^\mu}{(l^2)^2 l\nu} = 2iv^\mu \frac{1}{16\pi^2} \frac{\mu^\epsilon}{\epsilon} + \text{finite} \quad (140)$$

$$\mu^\epsilon \int \frac{d^{4-\epsilon}l}{(2\pi)^{4-\epsilon}} \frac{1}{l^2(l\nu)^2} = -4i \frac{1}{16\pi^2} \frac{\mu^\epsilon}{\epsilon} + \text{finite} \quad (141)$$

$$\mu^\epsilon \int \frac{d^{4-\epsilon}l}{(2\pi)^{4-\epsilon}} \frac{l^\mu l^\nu}{(l^2)^3} = \frac{i}{2} g^{\mu\nu} \frac{1}{16\pi^2} \frac{\mu^\epsilon}{\epsilon} + \text{finite} , \quad (142)$$

we can reduce the evaluation of our one-loop diagrams to algebra. The gluon insertion into a light-light current (cf. 4a) corresponds to the generic expression

$$\begin{aligned} I^{\mu} &= \mu^\epsilon \int \frac{d^{4-\epsilon}l}{(2\pi)^{4-\epsilon}} \frac{-ig_{\mu\nu}\delta_{ab}}{l^2} [-igT_a]_1^C \left[\gamma^\mu \frac{i}{\not{l}} \right]_1^D [-igT_b]_2^C \left[\gamma^\nu \frac{i}{\not{l}} \right]_2^D \\ &= -ig^2 \mu^\epsilon [T_a]_1^C [T_a]_2^C [\gamma^\mu \gamma^\alpha]_1^D [\gamma_\mu \gamma^\beta]_2^D \int \frac{d^{4-\epsilon}l}{(2\pi)^{4-\epsilon}} \frac{l_\alpha l_\beta}{(l^2)^3} \\ &= \frac{1}{2} \frac{\alpha}{4\pi} \frac{\mu^\epsilon}{\epsilon} [T_a]_1^C [T_a]_2^C [\gamma^\mu \gamma^\nu]_1^D [\gamma_\mu \gamma_\nu]_2^D + \text{finite} , \end{aligned} \quad (143)$$

where the notation $[S]_i^D$ refers to the insertion of the string S of Dirac matrices from right to left, starting at the appropriate vertex; similarly for $[S]_i^C$ in color space. I_{ll} has to be multiplied by -1 for each fermion line in which the charge flows in the opposite direction of the momentum.

The corresponding calculation for the heavy-light current (cf. 4b) yields

$$\begin{aligned}
I^{hl} &= \mu^\epsilon \int \frac{d^{4-\epsilon}l}{(2\pi)^{4-\epsilon}} \frac{-ig_{\mu\nu}\delta_{ab}}{l^2} [-igT_a]_h^C \left[v^\mu \frac{i}{lv} \right]_h^D [-igT_b]_l^C \left[\gamma^\nu \frac{i}{\not{l}} \right]_l^D \\
&= -ig^2 \mu^\epsilon [T_a]_h^C [T_a]_l^C [\not{\psi}\gamma^\alpha]_l^D \int \frac{d^{4-\epsilon}l}{(2\pi)^{4-\epsilon}} \frac{l_\alpha}{(l^2)^2(lv)} \\
&= 2\frac{\alpha}{4\pi} \frac{\mu^\epsilon}{\epsilon} [T_a]_h^C [T_a]_l^C + \text{finite} ,
\end{aligned} \tag{144}$$

where we have used $\not{\psi}\psi = 1$ in the last equality. Again, I_{hl} has to be multiplied by -1 for each fermion line in which the charge flows in the opposite direction of the momentum. There is a superficial ambiguity in the sign for heavy anti-quark lines. One possible rule is to treat them like anti-quarks; an equivalent one [9] is to treat them like quarks with the opposite color charge.

Finally the heavy-heavy current (cf. 4c) gives the contribution

$$\begin{aligned}
I^{hh} &= mu^\epsilon \int \frac{d^{4-\epsilon}l}{(2\pi)^{4-\epsilon}} \frac{-ig_{\mu\nu}\delta_{ab}}{l^2} [-igT_a]_1^C \left[v^\mu \frac{i}{lv} \right]_1^D [-igT_b]_2^C \left[v^\nu \frac{i}{lv} \right]_2^D \\
&= -ig^2 \mu^\epsilon [T_a]_1^C [T_a]_2^C \int \frac{d^{4-\epsilon}l}{(2\pi)^{4-\epsilon}} \frac{1}{(l^2)(lv)^2} \\
&= -4\frac{\alpha}{4\pi} \frac{\mu^\epsilon}{\epsilon} [T_a]_1^C [T_a]_2^C + \text{finite} ,
\end{aligned} \tag{145}$$

with the same rules for additional signs.

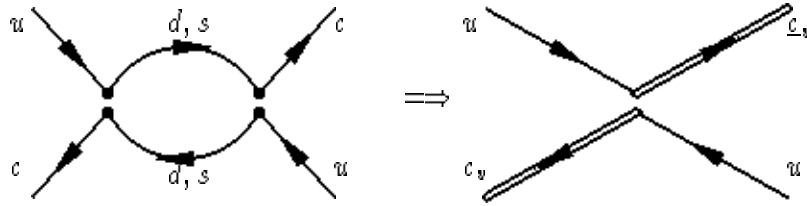


Figure 1: Matching of the four-quark operators at $\mu \approx m_c$

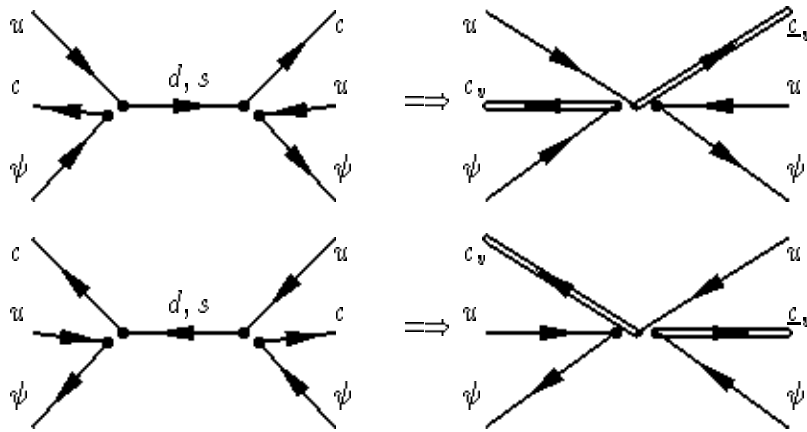


Figure 2: Six-quark matching

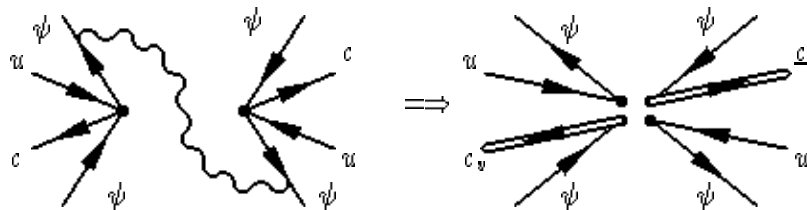


Figure 3: An example of a leading contribution to eight-quark matching. This graph corresponds to $(l:l::)$ in the notation of section ??.

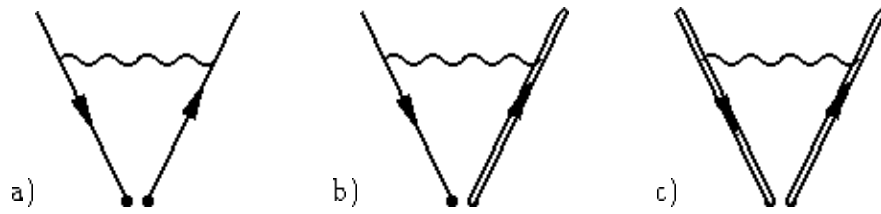


Figure 4: Gluon insertion into light-light, heavy-light, and heavy-heavy pairs of quark lines.

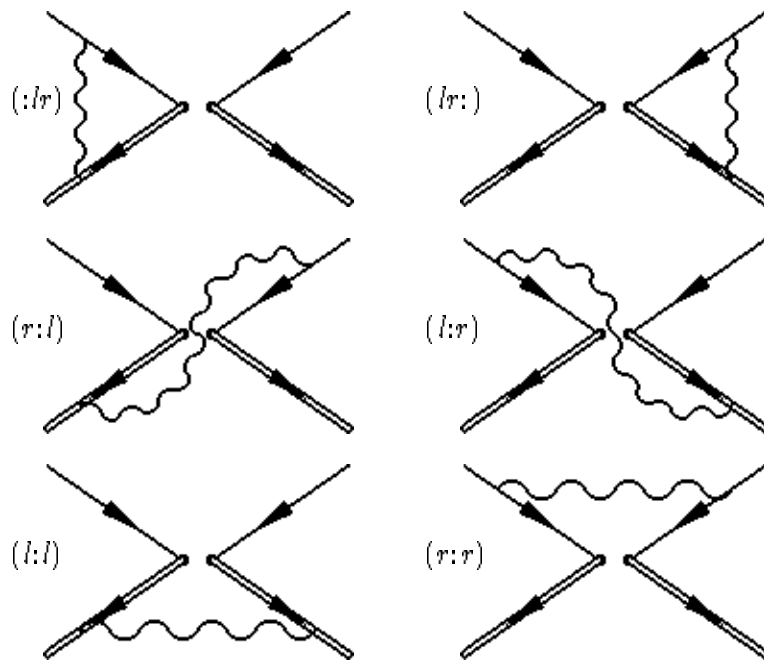


Figure 5: Running of the four-quark operators

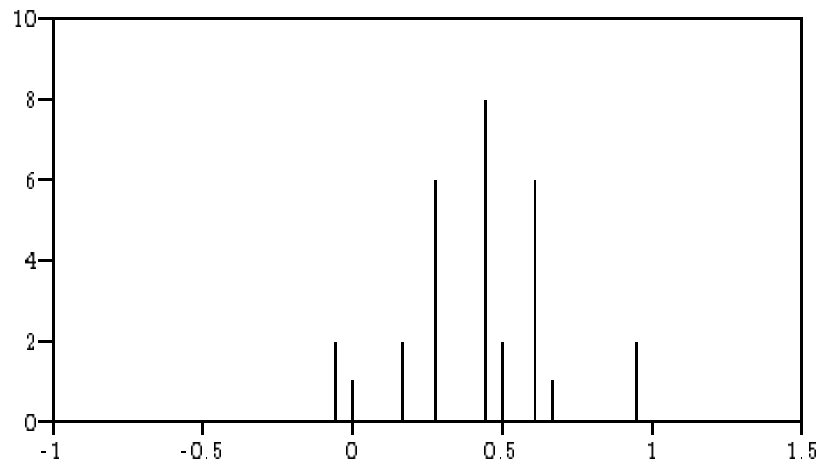


Figure 6: Multiplicity distribution of the eigenvalues of the anomalous dimension matrix $\tilde{\gamma}_6^D/18$ for the six-quark operators in the case $N = 3$.

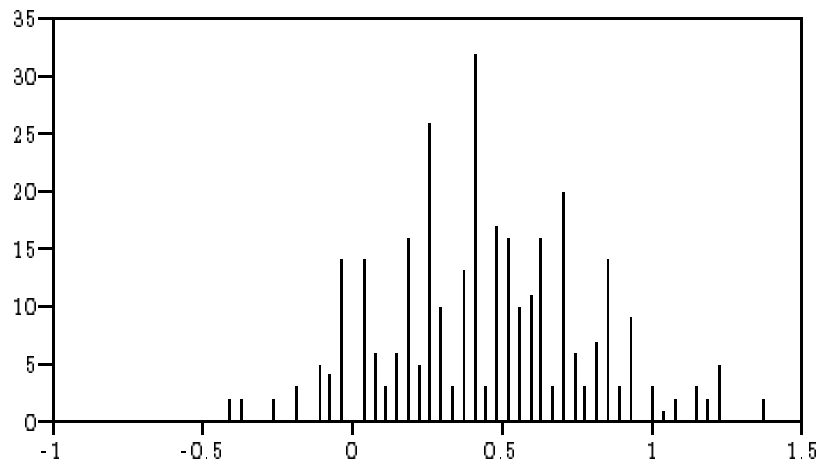


Figure 7: Multiplicity distribution of the eigenvalues of the anomalous dimension matrix $\tilde{\gamma}_8^D/18$ for the eight-quark operators in the case $N = 3$.